analytical chemistry

pubs.acs.org/ac Article

Nanodisc Reconstitution and Characterization of Amyloid-β Precursor Protein C99

Bankala Krishnarjuna,[▽] Gaurav Sharma,[▽] Volodymyr M. Hiiuk,[▽] Jochem Struppe, Pavel Nagorny, Magdalena I. Ivanova, and Ayyalusamy Ramamoorthy*

Cite This: *Anal. Chem.* 2024, 96, 9362−9369 Read Online

ACCESS | Metrics & More | Article Recommendations | Supporting Information

ABSTRACT: Amyloid precursor protein (APP) plays a pivotal role in the pathology of Alzheimer's disease (AD). Since the fragmentation of the membrane-bound APP that results in the production of amyloid-β peptides is the starting point for amyloid toxicity in AD, it is important to investigate the structure and dynamics of APP in a near-native lipid-bilayer environment. However, the reconstitution of APP into a stable and suitable membrane-mimicking lipid environment is a challenging task. In this study, the 99-residue C-terminal domain of APP is successfully reconstituted into polymer nanodiscs and characterized using size-exclusion chromatography, mass spectrometry, solution NMR, and magic-angle spinning solid-state NMR. In addition, the feasibility of using lipid-solubilizing polymers for isolating and characterizing APP in the native *Escherichia. coli* membrane environment is demonstrated.

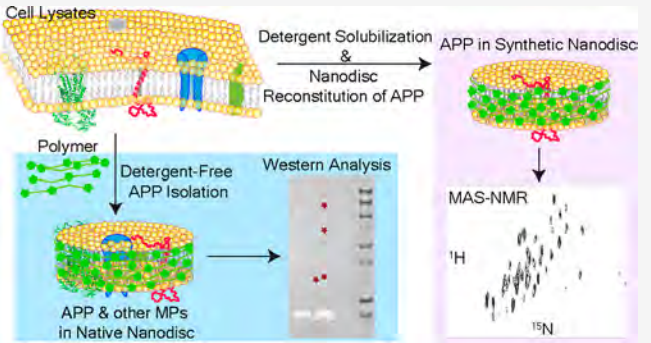

INTRODUCTION

Membrane proteins embedded in the cell membrane or anchored to the cell membrane play major roles in various cellular processes such as cell signaling, molecular transport, adhesion processes, and drug metabolism and, therefore, are primary targets for pharmaceutical drug development.[1−3] Hence, it is essential to explore the high-resolution structures of membrane proteins to understand the underlying molecular mechanism of their function and thus to assist drug design and development projects.[4−6] However, the *in vitro* characterization of membrane proteins is challenging, as their isolation/purification and, importantly, their reconstitution into a stable/suitable membrane-mimicking lipid environment are difficult in general.[7−10]

Although detergents are cost-effective and efficient in extracting membrane proteins, they have limitations, as their short alkyl chains and headgroups are chemically distinct from those of native membrane lipids, rendering them discrete physicochemical properties that can affect the function of membrane proteins.[5,11−13] Moreover, their denaturing properties make it difficult to maintain membrane protein's oligomeric or multimeric states that are stabilized by intermolecular interactions.[14−17] Planar lipid-bilayer-containing bicelles have been used extensively to study the structure, dynamics, and membrane topology of a variety of membrane proteins.[18] However, bicelles also contain detergent-like short-chain lipids that could affect the stability of a reconstituted membrane protein.[19−21] Likewise, liposomes are also limited by a lack of good stability and vesicular morphology.[9,22,23] Detergent-based membrane-mimicking systems offer minimal stability[13,24] and may not be desirable for high-resolution studies of membrane protein.[25,26] On the other hand, nanodiscs, which are nanometer-sized lipid bilayered systems surrounded and stabilized by a protective belt of peptides, proteins, or polymers , have been shown to provide a stable and more native-like membrane environment for studying the structure and function of various membrane proteins.[5,27−39]

This study aims to demonstrate the feasibility of using nanodiscs to study transmembrane protein domain C99 of the full-length amyloid precursor protein (APP). C99 plays an important role in the pathology of Alzheimer's disease (AD). APP is an integral membrane protein with 695−770 amino acid residues.[40] It is expressed in many different tissues, especially in the synapses of neurons, and its main biological function is yet to be understood.[41,42] However, APP is extensively studied in connection with its amyloid-β (Aβ) peptide, the key component of plaques in the pathogenesis of AD.[43−46] APP is non-systematically cleaved by secretases; thus, Aβ peptide fragments with different lengths are produced

Received: December 15, 2023
Revised: May 14, 2024
Accepted: May 22, 2024
Published: June 3, 2024

https://doi.org/10.1021/acs.analchem.3c05727
Anal. Chem. 2024, 96, 9362−9369

within the cell membrane.[47−49] The initial processing of APP by β-secretase results in a membrane-anchored C-terminal (99 residues) fragment (β-CTF) called C99 and a secreted fragment sAPPβ.[40,41] Further sequential processing of C99 by γ-secretase produces Aβ40 and Aβ42 peptide fragments within the cell membrane.[40,48] Previous studies have reported the importance of the lipid membrane and membrane composition on the structure and stability of the APP and C99. Therefore, to gain a molecular-level understanding of the processes underlying the production of Aβ peptides and the roles of the dynamic structure and membrane interaction of APP, it is essential to study APP (or C99) in a near-native lipid membrane.

A nonionic inulin functionalized with a hydrophobic pentyl group (pentyl-inulin) is used to prepare the nanodiscs to study C99.[50] Most of the reported nanodisc-forming synthetic polymers are ionic, and hence, they can interact with the desired membrane protein(s) to be reconstituted in nanodiscs, affecting their structure and function. Such undesired effects of the use of charged polymers have been reported for the positively charged cytochrome-P450 and the negatively charged cytochrome-b5 proteins, and the difficulty in functionally reconstituting P450-b5 complex.[51,52] A similar observation has been reported for the nanodisc-forming cationic-rich AEM28 peptide.[39] Thus, charged polymers/peptides are not suitable to study membrane proteins (or other biomolecules) that can exhibit electrostatic interactions with the nanodisc-forming polymers/peptides. To overcome these limitations, we developed a nonionic pentyl-inulin polymer by functionalizing inulin.[53] Therefore, in this study, the rationale for using the nonionic pentyl-inulin polymer is to avoid such nonspecific charge−charge interactions between the polymer belt and the target membrane protein and the lipid membrane.

C99 was overexpressed in *Escherichia coli* (BL21-C41strain) and solubilized using a pentyl-inulin polymer.[5,38,53,54] The polymer-solubilized APP in *E. coli* native lipids was characterized by sodium dodecyl sulfate polyacrylamide gel electrophoresis (SDS-PAGE) and Western blot. Protein was also purified under denaturing conditions and reconstituted into polymer nanodiscs (pentyl-inulin-based nanodiscs). The APP reconstituted in nanodiscs was characterized by size-exclusion chromatography (SEC), ^{1}H nuclear magnetic resonance (NMR) spectroscopy, dynamic-light scattering (DLS), differential scanning calorimetry (DSC), mass spectrometry, and transmission electron microscopy (TEM) experiments. A ^{15}N-labeled C99 expressed and purified from *E. coli* was also reconstituted into inulin-based polymer nanodiscs and characterized by high-resolution magic-angle spinning (MAS) solid-state NMR spectroscopy.

EXPERIMENTAL SECTION

Protein Expression. The plasmid (T7 promotor) expressing APP with a His_6-tag at the C-terminus (APP-C99) or APP with a His_{10}-tag at the N-terminus (APP-NT2) was transformed into C41-competent cells (Lucigen Corporation, WI, USA). After 16 h at 37 °C, a single colony from the transformation plate was inoculated into 10 mL of cells and grown overnight at 37 °C (starter culture). The protein was overexpressed by the autoinduction method, as previously reported.[55,56] Briefly, the starter culture was inoculated into ZYM-5052 autoinduction media [ZY—1% tryptone, 0.5% yeast extract; M—0.05 M KH_2PO_4, 0.05 M Na_2HPO_4, and 0.025 M $(NH_4)_2SO_4$, and 5052−0.5% glycerol, 0.05% glucose, and 0.2% lactose (pH 6.75)] containing 1 mM $MgSO_4$, 1× trace metal mix (Hollister, CA, USA), 0.1× Basal Medium Eagle vitamin (Sigma-Aldrich), and 100 μg/mL ampicillin, and were grown at 37 °C until the OD_{600} reached ∼0.8. Then the temperature was reduced to 20 °C, and the overexpression was allowed for 20 h. The cells were pelleted down by centrifugation at 6500g for 10 min at 4 °C and stored at −80 °C until protein solubilization/purification. For preparing ^{15}N-labeled C99 protein, $^{15}NH_4Cl$ was added to the buffers in the autoinduction media (1.5 g/L $^{15}NH_4Cl$, 0.005 M Na_2SO_4, 0.05 M KH_2PO_4, and 0.05 M Na_2HPO_4)

Cell Lysis and Membrane Preparation. Cells were resuspended in 10 mM Tris buffer (pH 7.4) containing 100 mM NaCl, lysozyme (5 mg/mL) (New Brunswick, NJ, USA), DNase (1 mg/mL) (Sigma-Aldrich, St. Louis, Missouri, USA), and 2 mM $MgCl_2$ (Sigma-Aldrich), and lysed by sonication using a 13 mm sonicator probe (Thomas Scientific, LLC, NJ) with 8 cycles of 10 s pulse and 1 min cooling between every 2 pulses. The soluble components were removed by centrifugation, and the membranes were collected and washed twice using the washing buffer [75 mM Tris at pH 7.8, 300 mM NaCl, 0.2 mM ethylenediaminetetraacetic acid (EDTA)]. To remove the EDTA, a third wash was done with resuspension buffer (10 mM Tris buffer, pH 7.4, and 100 mM NaCl). cOmplete protease inhibitor cocktail (Sigma-Aldrich) was included in all the steps of protein purification.

Pentyl-Inulin Synthesis. Natural inulin polymer extracted from chicory roots was purchased from Sigma-Aldrich. Pentyl-inulin (average molecular weight of ∼3 kDa) polymer used in this study was chemically synthesized by functionalizing inulin with hydrophobic pentyl groups using pentyl bromide (Sigma-Aldrich), purified, and characterized as described elsewhere.[53]

Membrane Solubilization Using Pentyl-Inulin. Cell membranes were weighed using an analytical balance and resuspended (25 mg/mL) in 10 mM Tris buffer (pH 7.4) containing 100 mM NaCl and mixed with polymer at a 1:1 w/w membrane-to-polymer ratio.[57] The solubilization was carried out at 4, 25, and 37 °C. Then, the insoluble components were removed by centrifugation at 10,000 rpm, 4 °C for 45 min. The clear supernatant was collected carefully for further analysis. In addition, as a control, the membranes were also solubilized in the presence of 0.5% *n*-dodecyl-beta-maltoside (DDM) detergent.

Western Blotting. SDS-PAGE was performed on the solubilized samples using 4−12% (gradient) bis-tris NuPAGE gel (Thermo Fisher Scientific, MA, USA). 1× MES NuPAGE was used as a gel running buffer. The gel was run at 100 V for 10 min and then at 120 V for 70 min at room temperature (RT). While running SDS-PAGE, the poly(vinylidene difluoride) (PVDF) membrane (Immuno-Blot Bio-Rad 1620177, 26 cm × 3.3 m, 0.2 μm) was soaked in 100% methanol for 30−60 min, followed by soaking in the transfer buffer (0.25 M Tris, 1.92 M glycine, and 20% methanol) for 5−10 min. Transfer from SDS-PAGE gel onto PVDF membrane was carried out at 4 °C and 110 V for 1 h. Then, the PVDF membrane was blocked with the blocking buffer [10% milk in TBST buffer −0.02 M Tris (pH 7.6), 0.15 M NaCl, and 0.1% Tween 20] for 1 h at RT. The blot was probed with the primary antibody (6E10; catalog no. 803004) (Bio Legend, San Diego, California, USA; prepared at a dilution of 1:500 in 5% milk TBST) and incubated overnight at 4 °C with gentle shaking. The next day, the membrane was washed three

https://doi.org/10.1021/acs.analchem.3c05727
Anal. Chem. 2024, 96, 9362−9369

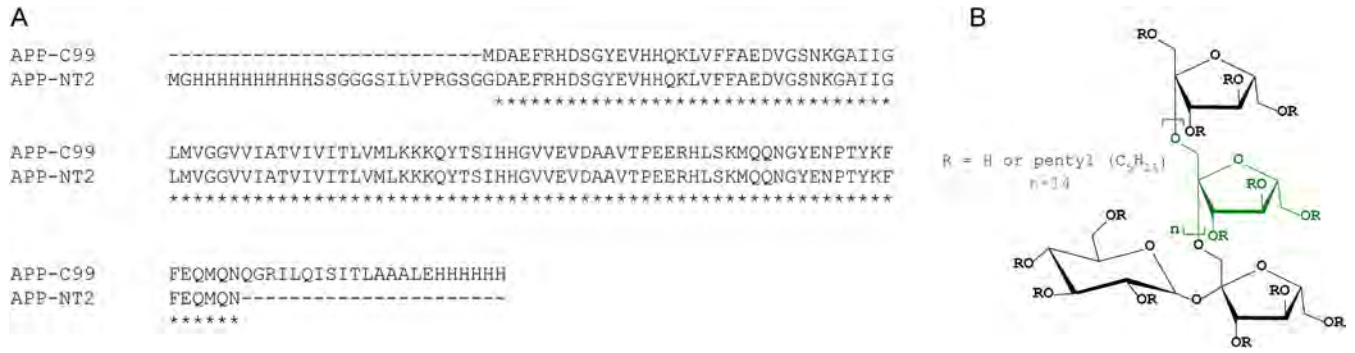

Figure 1. (A) Amino acid sequences of APP-C99 and APP-NT2. "*" Indicates the conserved residues. APP-NT2 has a His_{10}-tag, followed by a 14-residue-long linker sequence at the N-terminus. APP-C99 has a His_6-tag preceded by a 16-residue-long linker sequence at the C-terminus. (B) Chemical structure of inulin (fructooligosaccharides; $n \sim 14$) functionalized with pentyl groups.

times with 5% milk TBST before incubating with the secondary antibody (goat antimouse HRP, Thermo Fisher Scientific; cat. no. 32230; prepared at a dilution of 1:5000 in 5% milk TBST). The membrane was washed as previously, and the proteins were detected in the presence of a substrate, Eco bright Femto HRP.

Purification of APP-C99. The membranes were solubilized overnight in the solubilization buffer (20 mM Tris at pH 7.8, 150 mM NaCl, 8 M urea, 0.2% SDS) at 4 °C with gentle rotation. The insoluble material was removed by centrifugation at 39,000*g*, 4 °C for 30 min. The supernatant was collected and filtered using a 1.2 μm cellulose acetate filter (Findlay, OH, USA). Then, APP-C99 was purified by Ni-NTA affinity chromatography (Chicago, IL, USA). The sample was loaded onto a 5 mL Ni-NTA column equilibrated with the same solubilization buffer at a flow rate of 2 mL/min using FPLC. Then, the column was washed using 50 mL of 10 mM Tris buffer (pH 7.4) containing 100 mM NaCl and 3% Empigen BB (Sigma-Aldrich) to replace urea and SDS with Empigen. The APP-C99 was eluted from the column using an imidazole gradient (0−300 mM). The fractions from the elution peak (280 nm) were analyzed by SDS-PAGE (Piscataway, NJ, USA), and the fractions containing the APP-C99 protein were pooled. The concentration of APP-C99 was determined by UV spectroscopy using an extinction coefficient of 5960 M^{-1} cm^{-1}.

Preparation of Liposomes and Polymer Nanodiscs. 7 mg of DMPC and 3 mg of DMPG (Avanti Polar Lipids, Alabaster, USA) were dissolved in a 1:1 v/v in a CH_3OH/$CHCl_3$ solvent mixture. The solvents were removed by purging N_2 gas, followed by vacuum overnight. The dried lipids were resuspended in 10 mM Tris buffer (pH 7.4) containing 100 mM NaCl, and liposomes were made by using the freeze−thaw technique (3−5 cycles). Then, the liposomes were solubilized by mixing them with pentyl-inulin stock solution (100 mg/mL) at 1:1 w/w polymer/lipid ratio and incubating the sample overnight at 4 °C under gentle mixing. (Note: in the case of incomplete solubilization, 2−3 additional freeze−thaw cycles were performed to achieve complete solubilization of lipids.)

Reconstitution of APP-C99 into Polymer Nanodiscs. The solutions of 7:3 w/w DMPC/DMPG polymer nanodiscs, the detergent-purified APP-C99, and the Biobeads SM2 resin (Bio-Rad) were mixed and incubated at 4 °C for ∼4 h under slow/careful mixing using a magnetic bar. A 1:30 (w/w) detergent/biobeads ratio was used to remove the detergent for the APP-C99 reconstitution. The APP-C99-reconstituted nanodiscs were separated from the biobeads by filtration. The sample was then purified by SEC, and the fractions were analyzed by SDS-PAGE. The fractions containing the pure reconstituted protein were used for further characterization.

Mass Spectrometry. The molecular mass of the APP-C99 protein was determined by matrix-assisted laser desorption-ionization time-of-flight mass spectrometry (MALDI-TOF-MS). 1 μL of APP-C99 sample was pipetted on a 384 well MTP stainless-steel plate, followed by adding and mixing 1 μL of sinapic acid, α-cyano-4-hydroxycinnamic acid (CHCA), or 2,5-dihydroxybenzoic acid matrix. The samples were allowed to air-dry at room temperature before spectra were recorded on a Bruker Autoflex mass spectrometer under linear positive ion mode at a voltage of ∼19 kV. The instrument was calibrated in the midmass range, 5734.52−16952.31 Da, using insulin and myoglobin. The spectra were smoothened and corrected for baseline using FlexAnalysis version 3.4 software.

NMR Spectroscopy. All solution NMR experiments were performed on a Bruker 500 MHz NMR spectrometer (Billerica, MA, USA). One-dimensional ^{1}H NMR spectra were recorded from SEC-purified APP-C99 reconstituted in nanodiscs. The NMR data were processed and analyzed using Bruker TopSpin (version-3.6.2) software.

^{15}N isotope-labeled APP-C99 was also prepared and reconstituted in polymer nanodiscs. APP-C99 was concentrated by lyophilization, hydrated with water to a final volume of 30 μL (150 μM), and packed into a 3.2 mm NMR rotor. Two-dimensional (2D) [^{1}H−^{15}N]-HETCOR NMR spectra were recorded using 512 scans and 96 increments ($t1$ dimension) and a 2 s recycle delay. NMR data were collected on a 700SB MHz solid-state NMR spectrometer equipped with a 3.2 mm Efree HCN probe and facilitated with a VTN-type variable temperature unit. RF field strengths of 45 kHz on ^{1}H and 42.61 kHz on ^{15}N, and a 31.82 kHz frequency offset during cross-polarization (CP) on ^{1}H were used. The spectra were recorded at four different temperatures: 243, 253, 273, and 293 K. The success of the experiments is facilitated by the MAS technique with a 12.5 kHz MAS frequency. A 0.5 ms CP contact time was used to transfer magnetization from the proton to nitrogen. Chemical shifts were calibrated using MLF tripeptide as a ref 58.

Dynamic-Light Scattering. DLS measurements were carried out using a Wyatt Technology DynaPro NanoStar instrument equipped with a laser emitting at ∼662 nm. One μL of the SEC-purified nanodisc sample was loaded into the quartz MicroCuvette (Wyatt Technology, CA, USA). Ten acquisitions, each 5 s, were averaged to obtain the DLS profile.

https://doi.org/10.1021/acs.analchem.3c05727
Anal. Chem. 2024, 96, 9362−9369

All data were recorded at 25 °C, allowing for at least 10 min for the loaded sample temperature to equilibrate before data acquisition. The spectra were obtained in the mass-percentage mode.

Negative Stain Transmission Electron Microscopy. The carbon-coated copper 400 mesh TEM grids (Ted Pella, 01702 F) were activated by glow discharge for 45 s using the LEICA EM ACE600 SPUTTER COATER instrument. Five μL of nanodisc-reconstituted APP sample was adsorbed to the grids for 5 min at RT. The grids were washed twice with the Milli-Q and stained with 5 μL of 1% (w/v) uranyl acetate (Ted Pella Inc.). Excess uranyl acetate was blotted with the filter paper, and the grids were allowed to air-dry for ∼5 min. Grids with nanodiscs were imaged at a 120 kV accelerating voltage in a JEOL JEM 1400 PLUS electron microscope equipped with a NANOSPRT12 camera at a magnification of 50,000×.

Differential Scanning Calorimetry. DSC experiments were performed on a differential scanning calorimeter (DSC Nano, TA Instruments, New Castle, DE, USA) at a 1 °C/min scan rate under a constant pressure of 3 atm. Heating curves were obtained between the temperature range of 0−50 °C. The phase transition characterization was investigated for the 7:3 w/w DMPC/DMPG liposomes, protein-free polymer nanodiscs, and polymer nanodiscs reconstituted with APP-C99. The buffer alone was used to obtain the reference DSC profile and was subtracted from each sample type by using NanoAnalyze software. The buffers were filtered and degassed before use.

RESULTS AND DISCUSSION

The APP protein sequences used in this study are listed in Figure 1. C99 is the 99 amino acids containing the membrane-anchored region of the full-length APP. It has a C-terminal His_6 tag flanked by a 16-residue linker sequence (QGRILQI-SITLAAALE) (Figure 1A). The APP-NT2 is the same C99 construct but with an N-terminal His_{10}-tag flanked by a linker sequence.

Temperature-Dependent Solubilization of APP-Enriched *E. coli* Cell Membranes. The solubilization of APP-enriched bacterial cell membranes using pentyl-inulin (Figure 1B) was performed at three different temperatures: 4, 25, and 37 °C overnight. The protein band corresponding to APP-NT2 (∼13.9 kDa) was observed near 20 kDa size on the SDS-PAGE gel (Figure 2A). The unusual migration of the APP-NT2 protein on the SDS-PAGE gel might be due to the interference caused by the polymer and lipids present in the sample. Such unexpected migration of proteins is generally observed for some membrane proteins and also for highly hydrophilic (intrinsically disordered) proteins.[59] Another study reported that the change in the migration of the protein was due to differential interactions between protein and detergent (SDS) rather than between proteins,[60] which recommended other methods together with SDS-PAGE to confirm the size of the protein as well. Overall, the appearance of the APP-NT2 band in the soluble fraction indicates the successful solubilization of the APP-NT2-enriched membranes. Due to many *E. coli* protein bands overlapping with the target protein APP-NT2, it was difficult to resolve and visualize the APP-NT2 bands from solubilization at different temperatures. Therefore, the solubilized fractions containing APP-NT2 were further verified by Western-blot analysis.

Western Blot Confirmed the Presence of APP-NT2 in Polymer-Solubilized Cell Membranes. Western blot was performed on pentyl-inulin solubilized, APP-NT2-enriched *E. coli* cell membranes. 6E10 monoclonal antibody that is specific to the EFRHDS (3-8) sequence motif present within the N-terminal region of Aβ(1-16) was used to detect APP-NT2 in the polymer-solubilized *E. coli* cell membranes. Freshly dissolved Aβ42 was used as a positive control, which showed a clear band in the low-molecular-weight region as expected (Figures 2B and S1). The major protein band corresponding to APP-NT2 was detected in all three samples prepared at three different temperatures (Figures 2B and S1). However, there was a clear difference in the intensity of protein band between the three samples. The sample solubilized at 25 °C showed a strong band, followed by 4 and then 37 °C, indicating that the pentyl-inulin solubilized APP-NT2-rich *E. coli* membranes more effectively at 25 °C than 4 or 37 °C (Figures 2B and S1). Interestingly, the high temperature is not suitable for the solubilization of APP-enriched membranes by either pentyl-inulin or detergent (DDM). In addition, the intensity of protein bands from polymer samples was higher compared to the DDM-solubilized samples prepared at the same temperature conditions. These observations indicate that pentyl-inulin is more efficient in solubilizing APP-NT2-rich *E. coli* membranes than the commonly used DDM detergent. Strong protein bands were also observed in the insoluble fractions of the polymer-solubilized samples. Several low-intensity bands detected by 6E10 were also observed in the high-molecular-weight region, indicating some of the APP-NT2 was self-assembled into SDS-resistant dimeric and oligomeric species (Figures 2B and S1). Since APP is known to aggregate and oligomerize, it has been reported to show multiple bands on the gel[61,62] as reported for Aβ aggregation/oligomerization by *in vitro* biophysical/biochemical studies[63] and MD simulations.[64] These bands are more prominent in the polymer-solubilized samples compared to those in the DDM-solubilized samples (Figure 2B). The result also indicates the feasibility of pentyl-inulin for isolating challenging membrane-binding proteins like APP. Further optimization of solubilizing factors

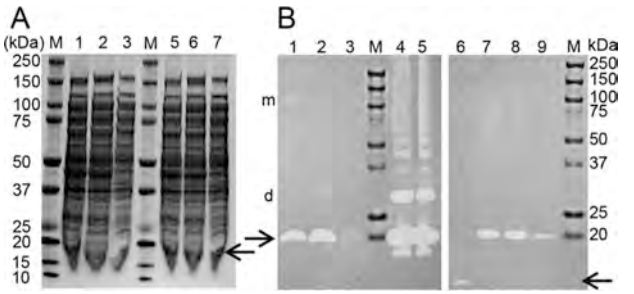

Figure 2. (A) Solubilization and SDS-PAGE analysis of APP-NT2-enriched *E. coli* cell membranes. M: protein molecular weight marker, Lanes; (1-3) and (5-7): APP-NT2-enriched membranes solubilized with pentyl-inulin at three different temperatures 4 °C (lanes; 1, 5), 25 °C (lanes; 2, 6), and 37 °C (lanes; 3, 7) (technical replicates). Protein band corresponding to APP-NT2 is indicated with an arrow. (B) Western-blot analysis of APP-NT2 in polymer and detergent-solubilized *E. coli* membranes. Lanes 1, 2, and 3 are the membranes solubilized by polymer at 4, 25, and 37 °C, respectively. Lanes 7, 8, and 9 are the membranes solubilized by DDM at 4, 25, and 37 °C, respectively. Lanes 4 and 5 were loaded with the insolubilized membrane components from DDM and polymer-solubilized samples, respectively. Lane 6: positive control; amyloid β42 M; and protein molecular weight marker. APP-NT2 and Aβ42 bands are indicated with arrows. Protein bands corresponding to dimer and multimer are indicated with d and m, respectively.

https://doi.org/10.1021/acs.analchem.3c05727
Anal. Chem. 2024, 96, 9362−9369

such as pH, metal ions, salt, and polymer concentration could be helpful to increase the yield of solubilized APP-C99.[57]

Detergent-Solubilization and Purification of APP-C99 Using Ni-NTA Affinity Chromatography. The *E. coli* membranes were solubilized overnight using 20 mM Tris pH 7.8, 150 mM NaCl, 8 M urea, and 0.2% SDS. The APP-C99 was purified using Ni-NTA affinity chromatography. The protein binding and the purification were done at room temperature. Prior to elution, the column was washed with 10 column volumes of imidazole-free buffer-containing Empigen. Then, the protein was eluted using different concentrations of imidazole. Most of the APP-C99 eluted at imidazole concentrations were higher than 80 mM (Figure S2). In addition, the impurities were minimal in these fractions. The protein band corresponding to APP-C99 was observed at a slightly higher molecular weight region (>15 kDa) than expected (13.78 kDa) (Figure S2). Such unusual migration of proteins on SDS-PAGE gels has been reported in the case of intrinsically disordered proteins.[65−67]

APP-C99 Is Successfully Reconstituted into Polymer Nanodiscs. 7:3 w/w DMPC/DMPG lipid ratio/composition was used to prepare stable nonionic polymer nanodiscs.[68] The APP-C99 fractions from Ni-NTA purification with minimum impurities were used for nanodisc reconstitution. The detergent (Empigen) was gradually removed using biobeads, and the reconstituted APP-C99 in polymer nanodiscs was purified by SEC. A major peak between 37−59 mL and a low-intensity peak between 100−123 mL were observed (Figure 3A). The fractions from the major peak were analyzed by SDS-PAGE. All of the fractions from the major peak showed a single pure protein band (Figure 3B). In the case of the polymer-solubilized sample, multiple protein bands were observed due to the oligomerization of APP-C99 (Figure 2B). But a single protein band observed for the detergent-purified and nanodisc-reconstituted APP-C99 sample indicates that inhibition or destabilization of self-assembled APP-C99 due to detergent exposure during purification and stabilization of the monomeric form of APP-C99 in nanodiscs.

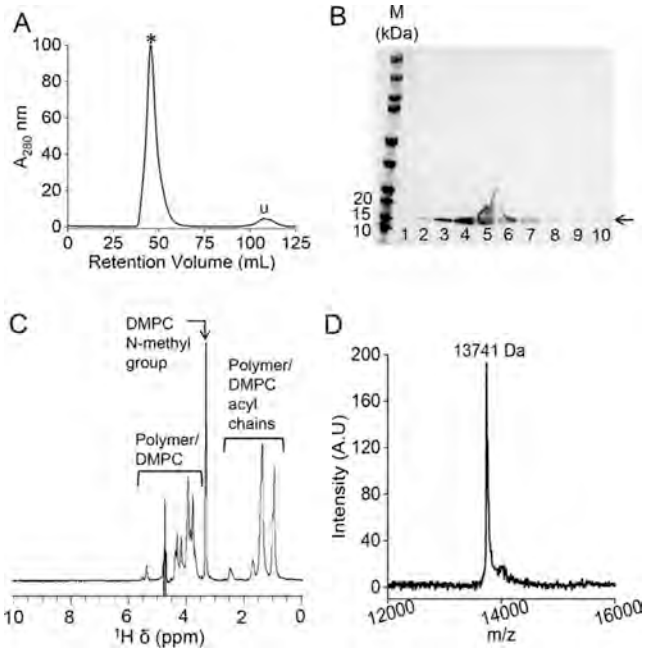

Figure 3. (A) Size-exclusion chromatography of nanodisc-reconstituted APP-C99. Elution peak corresponding to APP-C99 is indicated with a *. (B) SDS-PAGE analysis of the nanodisc-reconstituted APP-C99 fractions (1-10) collected from size-exclusion chromatography. Protein band corresponding to APP-C99 is indicated with an arrow. M denotes the protein marker. (C) ^{1}H NMR spectrum of polymer nanodisc-reconstituted APP-C99. Protein peaks are not prominent due to broadening caused by lipid-binding in nanodiscs. (D) MALDI-TOFF spectrum of APP-C99-reconstituted polymer nanodiscs.

^{1}H NMR and Mass Spectrometry. In the ^{1}H NMR spectrum, peaks corresponding to the lipids and polymer were observed (Figure 3C), but peaks from APP-C99 were not observed. The absence of protein signals is most likely due to line-broadening caused by the large size of the nanodiscs and the interaction of APP-C99 with DMPC/DMPG lipids in polymer nanodiscs. MS showed a major protein peak with 13741 Da, which is 30 Da less than the expected mass [13,771 Da; (PepCalc)] (Figure 3D). The observed mass difference is due to the sensitivity limitation of the instrument used to measure the molecular mass of the protein reconstituted in the nanodiscs. A low-intensity peak at ∼14,000 Da was also observed. The mass-to-charge ratio was acquired in a positive ion mode, and the observed high molecular mass species might be due to the formation of alkali metal ion adducts that are reported to occur with the CHCA matrix in a positive ion mode.[69] The observed higher mass could be due to the strong lipid binding to APP-C99.

Characterization by DLS, TEM, and DSC. The APP-C99-reconstituted polymer nanodiscs were further characterized using DLS and TEM for their size and size/shape, respectively. The measured hydrodynamic radius of APP nanodiscs using DLS was ∼9 ± 2 nm, indicating large-size particles present in solution (Figure 4A). This observation was in agreement with the early elution of polymer nanodiscs in SEC. Furthermore, TEM images indicated the nanodisc size as 20 ± 3 nm in diameter (Figure 4B). The morphology of the nanodiscs in the TEM image was nearly spherical, indicating that the integrity of the polymer nanodiscs was not affected by APP-C99 reconstitution.

The samples were also analyzed by DSC to see whether APP has any effect on the phase transition temperature of the lipids in polymer nanodiscs (Figure 4C). The observed T_m for the 7:3 w/w DMPC/DMPG liposomes (reference) was 23.4 °C. In contrast, the T_m for the 7:3 (w/w) DMPC/DMPG in polymer nanodisc-reconstituted with APP-C99 was 26.6 °C, which is 3.2 °C higher than that observed for DMPC liposomes. The T_m for the protein-free nanodiscs was similar to that of protein-reconstituted nanodiscs (Figure 4C), indicating that the C99 binding did not substantially affect the 7:3 (w/w) DMPC/DMPG lipid order in polymer nanodiscs. The pretransition/ripple phase peak observed at 14 °C for the DMPC liposomes was not observed for the APP-C99-reconstituted polymer nanodiscs (Figure 4C). The absence of a pretransition peak was due to the stable bilayer arrangement of lipids in polymer nanodiscs, restricting the tilting of lipid acyl chains. In addition, the phase-transition peaks of polymer nanodiscs with and without APP-C99 were broadened substantially than that observed for the 7:3 (w/w) DMPC/DMPG liposomes. The line-broadening and a higher T_m observed for the polymer nanodiscs with and without APP-C99 indicate a noncooperative behavior of lipids due to the increased order facilitated by polymer interaction as a stabilizing lipid bilayer belt. Moreover, the interaction of

https://doi.org/10.1021/acs.analchem.3c05727
Anal. Chem. 2024, 96, 9362−9369

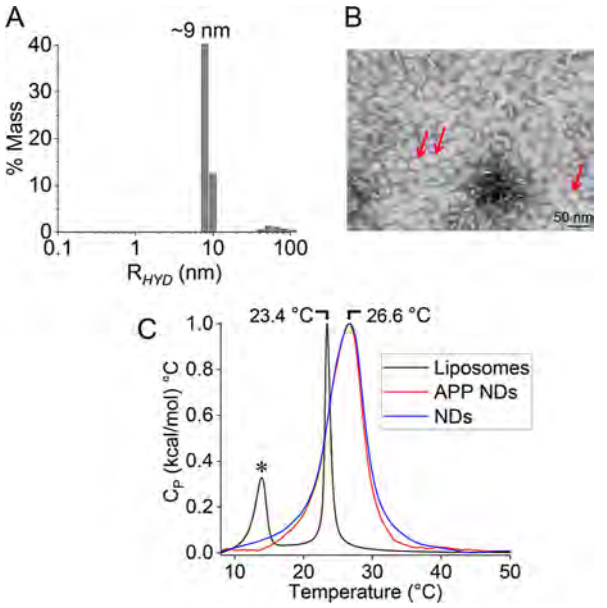

Figure 4. APP-C99-reconstituted 7:3 w/w DMPC/DMPG polymer nanodiscs were analyzed by (A) DLS, (B) TEM, and (C) DSC measurements. Reference DSC profiles were recorded using 7:3 w/w DMPC/DMPG liposomes (C; black) and 7:3 w/w DMPC/DMPG polymer nanodiscs (C; blue) and compared with C99-reconstituted 7:3 w/w DMPC/DMPG polymer nanodiscs (C; red). TEM image shows face-on and edge-on (bottom) sides of nanodiscs (~20 nm diameter). Well-resolved nanodiscs used to measure the nanodisc diameter are indicated with red arrows. Pretransition peak (14 °C) observed for the liposomes in DSC profile is indicated with a "*".

APP with DMPC/DMPG may also be attributed to the change in the physical phase behavior of lipids in the polymer nanodiscs. However, no substantial difference was observed in the T_m of polymer nanodiscs with and without APP-C99 (Figure 4C).

Polymer Nanodiscs Are Feasible for High-Resolution Solid-State NMR Studies of APP-C99. Previously, the APP was characterized in lyso-myristoylphosphatidylglycerol detergent micelles using solution NMR spectroscopy.[70] MD simulations suggests micelles influence the helical conformation of APP.[71] The dimer with the right-handed coiled-coil conformation is dominant in 1-palmitoyl-2-oleoylphosphatidylcholine bilayers, whereas the dimer with a left-handed conformation was observed in dodecylphosphocholine micelles.[72,73] These observations signify the importance of the native membrane environment for the structural studies of membrane proteins in general. In this study, we wanted to examine how reconstitution into lipid-bilayer affects the quality of the NMR spectrum. 150 μM ^{15}N-isotope-labeled APP-C99 was reconstituted in 7:3 (w/w) DMPC/DMPG polymer nanodiscs and characterized by solid-state NMR spectroscopy under MAS conditions (Figure 5). Since the amount of protein (150 μM) present in the 30 μL nanodisc sample in the 3.2 mm rotor is very small, it is a challenge to obtain high quality NMR spectra for APP-C99. The 2D spectrum displays well resolved ^{15}N−^{1}H resonances. By use of a short CP contact time, resonances from immobile residues of the protein that possess strong ^{1}H−^{15}N dipolar couplings can be selectively observed. On the other hand, residues from the soluble domain of the protein are expected to undergo faster motion as compared to transmembrane/membrane-bound residues and therefore

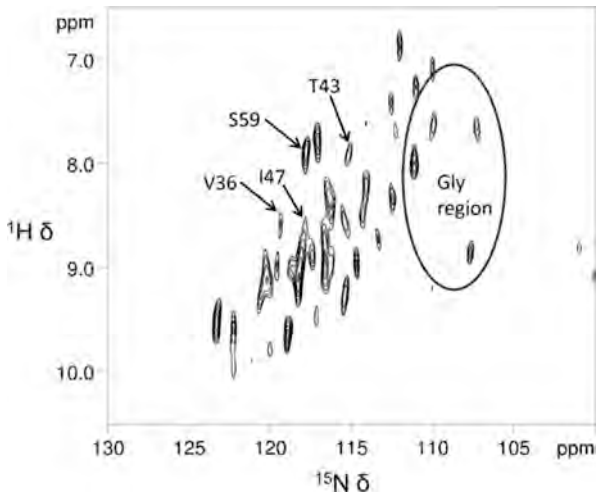

Figure 5. 2D [^{1}H−^{15}N]-HETCOR NMR spectrum of APP-C99 reconstituted into 7:3 w/w DMPC/DMPG polymer nanodiscs. The spectrum was recorded on a 700 MHz Bruker NMR spectrometer at 293 K. A 0.5 s CP contact time was used to detect lipid embedded/bound amino acid residues of APP-C99. Partial assignments are shown. 30 μL of 150 μM APP-C99 reconstituted in 7:3 (w/w) DMPC/DMPG polymer nanodiscs and 10 mM potassium phosphate buffer (pH 7.4) was packed into 3.2 mm MAS NMR rotor.

require a longer CP contact time as they are associated with weak motionally averaged ^{1}H−^{15}N dipolar couplings. Therefore, with 0.5 s CP contact time used in acquiring the 2D spectrum, most of the observed resonances are expected to be from the lipid bilayer-embedded amino acid residues and those making strong contacts with the lipid bilayer surface of the nanodisc. However, due to the extensive overlap of resonances, only a few NMR assignments were made based on the chemical shifts reported in the literature.[70] The spectral broadening observed in the current study is substantially large compared to that reported in micelles/bicelles.[70] Peak overlap became severe at lower temperature (243−273 K) likely due to the less dynamic gel phase of lipids (Figure S3). The increased peak broadening observed in nanodiscs is due to the large size (~20 nm diameter) of nanodiscs and also due to the low temperature conditions (273−243 K) used to record NMR spectra. Overall, the NMR data suggests the feasibility of using high-resolution solid-state NMR to characterize APP-C99 in polymer nanodiscs in future studies. Further enhancement of resolution can be achieved by using deuterated lipids and faster MAS experiments. Assignment of resonances and structure determination can be accomplished by employing 3D MAS experiments and using ^{13}C−^{15}N-labeled proteins and deuterated lipids as needed.

CONCLUSIONS

In this study, we have successfully demonstrated the direct isolation and reconstitution of APP-C99 in pentyl-inulin polymer-based nanodiscs. We have also successfully reconstituted detergent-purified APP-C99 in 7:3 (w/w) DMPC/DMPG pentyl-inulin polymer nanodiscs. The APP-C99-reconstituted nanodiscs were characterized by a combination of SEC, DLS, and TEM measurements that revealed stable and homogeneous size nanodiscs. The presence of APP-C99 did not substantially influence the physical behavior of lipids encased in the polymer nanodiscs. Moreover, the feasibility of isolating APP-C99 in native lipids using a polymer is

https://doi.org/10.1021/acs.analchem.3c05727
Anal. Chem. 2024, 96, 9362−9369

demonstrated. Room temperature is shown to be more effective for the polymer-based solubilization of APP-C99-enriched bacterial cell membranes. Solid-state NMR spectra acquired under MAS conditions indicated the feasibility of using polymer nanodiscs for high-resolution structural and dynamical studies of APP-C99.

■ ASSOCIATED CONTENT

Supporting Information

The Supporting Information is available free of charge at https://pubs.acs.org/doi/10.1021/acs.analchem.3c05727.

Western blot, SDS-PAGE, and 2D NMR (PDF)

■ AUTHOR INFORMATION

Corresponding Author

Ayyalusamy Ramamoorthy − *Biophysics Program, University of Michigan, Ann Arbor, Michigan 48109, United States; Department of Chemistry, Biomedical Engineering, Macromolecular Science and Engineering, University of Michigan, Ann Arbor, Michigan 48109, United States; National High Magnetic Field Laboratory and Department of Chemical and Biomedical Engineering, FAMU-FSU College of Engineering, Florida State University, Tallahassee, Florida 32310, United States;* orcid.org/0000-0003-1964-1900; Email: aramamoorthy@fsu.edu, ramamoor@umich.edu

Authors

Bankala Krishnarjuna − *Biophysics Program, University of Michigan, Ann Arbor, Michigan 48109, United States; Department of Chemistry, Biomedical Engineering, Macromolecular Science and Engineering, University of Michigan, Ann Arbor, Michigan 48109, United States;* orcid.org/0000-0002-4575-0011

Gaurav Sharma − *Biophysics Program, University of Michigan, Ann Arbor, Michigan 48109, United States; Department of Chemistry, Biomedical Engineering, Macromolecular Science and Engineering, University of Michigan, Ann Arbor, Michigan 48109, United States*

Volodymyr M. Hiiuk − *Biophysics Program, University of Michigan, Ann Arbor, Michigan 48109, United States; Department of Chemistry, University of Michigan, Ann Arbor, Michigan 48109, United States*

Jochem Struppe − *Bruker Biospin Corporation, Billerica, Massachusetts 01821, United States;* orcid.org/0000-0001-9001-5991

Pavel Nagorny − *Department of Chemistry, University of Michigan, Ann Arbor, Michigan 48109, United States;* orcid.org/0000-0002-7043-984X

Magdalena I. Ivanova − *Biophysics Program, University of Michigan, Ann Arbor, Michigan 48109, United States; Department of Neurology, University of Michigan, Ann Arbor, Michigan 48109, United States*

Complete contact information is available at: https://pubs.acs.org/10.1021/acs.analchem.3c05727

Author Contributions

[▽]B.K., G.S., and V.M.H. contributed equally.

Notes

The authors declare no competing financial interest.

■ ACKNOWLEDGMENTS

This study was supported by the National Institutes of Health (NIH) (R35 GM139572 and RO1 DK132214 to A.R. and R35 GM136341 to P.N.). We thank Dr. Thirupathi Ravula for help with the synthesis of the pentyl-inulin polymer used in this study, and Professor Charles Sanders from the Department of Biochemistry, Vanderbilt University School of Medicine for kindly providing the APP plasmid constructs.

■ REFERENCES

(1) Gulezian, E.; Crivello, C.; Bednenko, J.; Zafra, C.; Zhang, Y.; Colussi, P.; Hussain, S. *Trends Pharmacol. Sci.* **2021**, *42*, 657−674.
(2) Levental, I.; Lyman, E. *Nat. Rev. Mol. Cell Biol.* **2023**, *24*, 107−122.
(3) Piper, S. J.; Johnson, R. M.; Wootten, D.; Sexton, P. M. *Chem. Rev.* **2022**, *122*, 13989−14017.
(4) Overington, J. P.; Al-Lazikani, B.; Hopkins, A. L. *Nat. Rev. Drug Discovery* **2006**, *5*, 993−996.
(5) Krishnarjuna, B.; Ramamoorthy, A. *Biomolecules* **2022**, *12*, 1076.
(6) Young, J. W. *Biochem. Soc. Trans.* **2023**, *51*, 1405−1416.
(7) Bayburt, T. H.; Grinkova, Y. V.; Sligar, S. G. *Nano Lett.* **2002**, *2*, 853−856.
(8) Ritchie, T. K.; Grinkova, Y. V.; Bayburt, T. H.; Denisov, I. G.; Zolnerciks, J. K.; Atkins, W. M.; Sligar, S. G. *Methods Enzymol.* **2009**, *464*, 211−231.
(9) Bayburt, T. H.; Sligar, S. G. *FEBS Lett.* **2010**, *584*, 1721−1727.
(10) Shen, H. H.; Lithgow, T.; Martin, L. *Int. J. Mol. Sci.* **2013**, *14*, 1589−1607.
(11) Yeung, Y.-G.; Stanley, E. R. *Curr. Protoc. Protein Sci.* **2010**, *59*, 16.12.1−16.12.5.
(12) Bao, H.; Dalal, K.; Wang, V.; Rouiller, I.; Duong, F. *Biochim. Biophys. Acta, Biomembr.* **2013**, *1828*, 1723−1730.
(13) Yang, Z.; Wang, C.; Zhou, Q.; An, J.; Hildebrandt, E.; Aleksandrov, L. A.; Kappes, J. C.; DeLucas, L. J.; Riordan, J. R.; Urbatsch, I. L.; et al. *Protein Sci.* **2014**, *23*, 769−789.
(14) Seddon, A. M.; Curnow, P.; Booth, P. J. *Biochim. Biophys. Acta, Biomembr.* **2004**, *1666*, 105−117.
(15) Lambert, N. A. *Sci. Signal.* **2010**, *3*, pe12.
(16) Marty, M. T.; Hoi, K. K.; Robinson, C. V. *Acc. Chem. Res.* **2016**, *49*, 2459−2467.
(17) Young, J. W.; Wason, I. S.; Zhao, Z.; Kim, S.; Aoki, H.; Phanse, S.; Rattray, D. G.; Foster, L. J.; Babu, M.; Duong van Hoa, F. *J. Proteome Res.* **2022**, *21*, 1748−1758.
(18) Dürr, U. H. N.; Gildenberg, M.; Ramamoorthy, A. *Chem. Rev.* **2012**, *112*, 6054−6074.
(19) Lucyanna, B.-B.; Gelen, R.; Merce, C.; Laia, R.; Carmen, L.-I.; Alfons, D. l. M.; Olga, L. *Pharmaceutics* **2011**, *3* (3), 636−664.
(20) Majeed, S.; Ahmad, A. B.; Sehar, U.; Georgieva, E. R. *Membranes* **2021**, *11*, 685.
(21) Thoma, J.; Burmann, B. M. *Int. J. Mol. Sci.* **2020**, *22*, 50.
(22) Isalomboto Nkanga, C.; Murhimalika Bapolisi, A.; Ikemefuna Okafor, N.; Werner Maçedo Krause, R. *General Perception of Liposomes: Formation, Manufacturing and Applications*; IntechOpen, 2019..
(23) Zhang, J.-X.; Wang, K.; Mao, Z. F.; Fan, X.; Jiang, D. L.; Chen, M.; Cui, L.; Sun, K.; Dang, S. C. *Int. J. Nanomed.* **2013**, *8*, 1325−1334.
(24) Carlson, M. L.; Young, J. W.; Zhao, Z.; Fabre, L.; Jun, D.; Li, J.; Li, J.; Dhupar, H. S.; Wason, I.; Mills, A. T.; et al. *eLife* **2018**, *7*, No. e34085.
(25) Cross, T. A.; Sharma, M.; Yi, M.; Zhou, H. X. *Trends Biochem. Sci.* **2011**, *36*, 117−125.
(26) Das, B. B.; Nothnagel, H. J.; Lu, G. J.; Son, W. S.; Tian, Y.; Marassi, F. M.; Opella, S. J. *J. Am. Chem. Soc.* **2012**, *134*, 2047−2056.
(27) Kijac, A. Z.; Li, Y.; Sligar, S. G.; Rienstra, C. M. *Biochemistry* **2007**, *46*, 13696−13703.
(28) Luthra, A.; Gregory, M.; Grinkova, Y. V.; Denisov, I. G.; Sligar, S. G. *Methods Mol. Biol.* **2013**, *987*, 115−127.

(29) Hagn, F.; Etzkorn, M.; Raschle, T.; Wagner, G. *J. Am. Chem. Soc.* **2013**, *135*, 1919−1925.
(30) Denisov, I. G.; Sligar, S. G. *Nat. Struct. Mol. Biol.* **2016**, *23*, 481−486.
(31) Denisov, I. G.; Sligar, S. G. *Chem. Rev.* **2017**, *117*, 4669−4713.
(32) Nasr, M. L.; Baptista, D.; Strauss, M.; Sun, Z. Y. J.; Grigoriu, S.; Huser, S.; Plückthun, A.; Hagn, F.; Walz, T.; Hogle, J. M.; et al. *Nat. Methods* **2017**, *14*, 49−52.
(33) Hagn, F.; Nasr, M. L.; Wagner, G. *Nat. Protoc.* **2018**, *13*, 79−98.
(34) Nasr, M. L.; Wagner, G. *Curr. Opin. Struct.* **2018**, *51*, 129−134.
(35) Sligar, S. G.; Denisov, I. G. *Protein Sci.* **2021**, *30*, 297−315.
(36) Zhang, M.; Gui, M.; Wang, Z.-F.; Gorgulla, C.; Yu, J. J.; Wu, H.; Sun, Z.-Y. J.; Klenk, C.; Merklinger, L.; Morstein, L.; et al. *Nat. Struct. Mol. Biol.* **2021**, *28*, 258−267.
(37) Janata, M.; Gupta, S.; Čadová, E.; Angelisová, P.; Krishnarjuna, B.; Ramamoorthy, A.; Hořejší, V.; Raus, V. *Eur. Polym. J.* **2023**, *198*, 112412.
(38) Krishnarjuna, B.; Im, S. C.; Ravula, T.; Marte, J.; Auchus, R. J.; Ramamoorthy, A. *Anal. Chem.* **2022**, *94*, 11908−11915.
(39) Krishnarjuna, B.; Sharma, G.; Im, S.-C.; Auchus, R.; Anantharamaiah, G. M.; Ramamoorthy, A. *J. Colloid Interface Sci.* **2024**, *653*, 1402−1414.
(40) Chen, G. F.; Xu, T. H.; Yan, Y.; Zhou, Y. R.; Jiang, Y.; Melcher, K.; Xu, H. E. *Acta Pharmacol. Sin.* **2017**, *38*, 1205−1235.
(41) Zheng, H.; Koo, E. H. *Mol. Neurodegener.* **2011**, *6*, 27.
(42) van der Kant, R.; Goldstein, L. S. *Dev. Cell* **2015**, *32*, 502−515.
(43) Shen, J.; Kelleher, R. J., III *Proc. Natl. Acad. Sci. U.S.A.* **2007**, *104*, 403−409.
(44) Beel, A. J.; Sakakura, M.; Barrett, P. J.; Sanders, C. R. *Biochim. Biophys. Acta, Mol. Cell Biol. Lipids* **2010**, *1801*, 975−982.
(45) Lane, C. A.; Hardy, J.; Schott, J. M. *Eur. J. Neurol.* **2018**, *25*, 59−70.
(46) Sehar, U.; Rawat, P.; Reddy, A. P.; Kopel, J.; Reddy, P. H. *Int. J. Mol. Sci.* **2022**, *23*, 12924.
(47) Haass, C.; Kaether, C.; Thinakaran, G.; Sisodia, S. *CSH Perspect. Med.* **2012**, *2*, a006270.
(48) Capone, R.; Tiwari, A.; Hadziselimovic, A.; Peskova, Y.; Hutchison, J. M.; Sanders, C. R.; Kenworthy, A. K. *J. Biol. Chem.* **2021**, *296*, 100652.
(49) Pfundstein, G.; Nikonenko, A. G.; Sytnyk, V. *Front. Dell Dev. Biol.* **2022**, *10*, 969547.
(50) Ramamoorthy, A.; Ravula, T. Lipid nanodisc formation by polysaccharides modified with hydrophobic groups. U.S. Patent 18,029,064, 2023.
(51) Ravula, T.; Hardin, N. Z.; Bai, J.; Im, S. C.; Waskell, L.; Ramamoorthy, A. *ChemComm* **2018**, *54*, 9615−9618.
(52) Krishnarjuna, B.; Ravula, T.; Ramamoorthy, A. *ChemComm* **2020**, *56*, 6511−6514.
(53) Ravula, T.; Ramamoorthy, A. *Angew. Chem., Int. Ed.* **2021**, *60*, 16885−16888.
(54) Krishnarjuna, B.; Ravula, T.; Ramamoorthy, A. *ChemComm* **2022**, *58*, 4913−4916.
(55) Studier, F. W. *Protein Expression Purif.* **2005**, *41*, 207−234.
(56) Bentley, M. R.; Ilyichova, O. V.; Wang, G.; Williams, M. L.; Sharma, G.; Alwan, W. S.; Whitehouse, R. L.; Mohanty, B.; Scammells, P. J.; Heras, B.; et al. *J. Med. Chem.* **2020**, *63*, 6863−6875.
(57) Krishnarjuna, B.; Sharma, G.; Ravula, T.; Ramamoorthy, A. *Biochim. Biophys. Acta, Biomembr.* **2024**, *1866*, 184240.
(58) Kumari, B.; Brodrecht, M.; Gutmann, T.; Breitzke, H.; Buntkowsky, G. *Appl. Magn. Reson.* **2019**, *50*, 1399−1407.
(59) Rath, A.; Glibowicka, M.; Nadeau, V. G.; Chen, G.; Deber, C. M. *Proc. Natl. Acad. Sci. U.S.A.* **2009**, *106*, 1760−1765.
(60) Walkenhorst, W. F.; Merzlyakov, M.; Hristova, K.; Wimley, W. C. *Biochim. Biophys. Acta, Biomembr.* **2009**, *1788*, 1321−1331.
(61) Gerber, H.; Wu, F.; Dimitrov, M.; Garcia Osuna, G. M.; Fraering, P. C. *J. Biol. Chem.* **2017**, *292*, 3751−3767.
(62) Perrin, F.; Papadopoulos, N.; Suelves, N.; Opsomer, R.; Vadukul, D. M.; Vrancx, C.; Smith, S. O.; Vertommen, D.; Kienlen-Campard, P.; Constantinescu, S. N. *iScience* **2020**, *23*, 101887.
(63) Fawzi, N. L.; Ying, J.; Ghirlando, R.; Torchia, D. A.; Clore, G. M. *Nature* **2011**, *480*, 268−272.
(64) Okumura, H.; Itoh, S. G. *Molecules* **2022**, *27*, 2483.
(65) MacRaild, C. A.; Zachrdla, M.; Andrew, D.; Krishnarjuna, B.; Nováček, J.; Žídek, L.; Sklenář, V.; Richards, J. S.; Beeson, J. G.; Anders, R. F.; et al. *PLoS One* **2015**, *10*, No. e0119899.
(66) Morales, R. A. V.; MacRaild, C. A.; Seow, J.; Krishnarjuna, B.; Drinkwater, N.; Rouet, R.; Anders, R. F.; Christ, D.; McGowan, S.; Norton, R. S. *Sci. Rep.* **2015**, *5*, 10103.
(67) Krishnarjuna, B.; Andrew, D.; MacRaild, C. A.; Morales, R. A. V.; Beeson, J. G.; Anders, R. F.; Richards, J. S.; Norton, R. S. *Sci. Rep.* **2016**, *6*, 20613.
(68) Krishnarjuna, B.; Marte, J.; Ravula, T.; Ramamoorthy, A. *J. Colloid Interface Sci.* **2023**, *634*, 887−896.
(69) Lou, X.; Miley, G.; Van Dongen, J. L. J. *Rapid Commun. Mass Spectrom.* **2021**, *35*, No. e9111.
(70) Barrett, P. J.; Song, Y.; Van Horn, W. D.; Hustedt, E. J.; Schafer, J. M.; Hadziselimovic, A.; Beel, A. J.; Sanders, C. R. *Science* **2012**, *336*, 1168−1171.
(71) Dominguez, L.; Meredith, S. C.; Straub, J. E.; Thirumalai, D. *J. Am. Chem. Soc.* **2014**, *136*, 854−857.
(72) Nadezhdin, K. D.; Bocharova, O. V.; Bocharov, E. V.; Arseniev, A. S. *FEBS Lett.* **2012**, *586*, 1687−1692.
(73) Dominguez, L.; Foster, L.; Straub, J. E.; Thirumalai, D. *Proc. Natl. Acad. Sci. USA* **2016**, *113*, E5281−E5287.

https://doi.org/10.1021/acs.analchem.3c05727
Anal. Chem. 2024, 96, 9362−9369